TECHNICAL DIAGNOSTICS OF HYDRAULIC ROTATOR

TOMAS BUDIK, ROBERT JANKOVYCH

Brno University of Technology, Faculty of Mechanical Engineering, Institute of Production Machines, Systems and Robotics, Brno, Czech Republic

This article deals with the design of a technical diagnostics system for hydraulic rotators and the successful implementation of a unique hydraulic test bench. Based on an analysis of the design and function of all types of hydraulic rotators available on the world market, a system of requirements for the test bench and its place in the test centre was formulated. Furthermore, four diagnostic parameters from the group of deformation diagnostics and hydraulic systems diagnostics are proposed and used to evaluate the technical condition of the Indexator IR25 hydraulic rotator. For the evaluation of individual parameter values, a modified Shewhart control chart method is proposed for individual values and moving ranges of each parameter. Based on the measurements of 30 rotators, control limits were designed for statistical evaluation of the technical condition of the mentioned hydraulic rotator.

1 INTRODUCTION

The hydraulic rotator (hereinafter referred to as HR or rotator) belongs to the category of slow-running hydraulic equipment, which reaches approximately of 30 rpm at relatively high mechanical load conditions. The torques developed by the HR are in the thousands of N.m and the possible axial load in the hundreds of kN. For this reason, it is relatively difficult to measure these parameters and a very robust measuring device is required to transfer these loads **[Cerha 2010], [Vacca 2021], [Dell 2015], [Gotz 1998], [Singh 2017], [Khalil 2016], [Zhang 2019]**.

Currently, according to the available information, there is no equipment on the market that can multiparametrically investigate the technical condition of the entire rotator. The test benches that are currently published in the public sources only focus on certain parameters that do not meet the conditions for complex HR testing **[Onderka 2014], [Argo-Hytos Protech 2022], [Hycom 2022], [MH Hydraulics Netherlands 2022]**.

Researchers at Luleå University of Technology in Sweden worked on Rotator assembly at Indexator in 2016-2017. In the thesis [Lundström 2017], the authors have designed a workstation to make HR assembly more productive, and the thesis concludes with a simplified design of a test bench to test functionality after assembly. The proposed test bench does not meet the complex requirements proposed in the following chapters for HR testing. Manufacturers of test stands include Argo Hytos, Bosch Rexroth, Hydac, but they do not publish details of their research in this area **[Argo-Hytos 2022], [Bosch Rexroth 2022], [Hydac 2022], [MH Hydraulics Netherlands 2022], [Hycom 2022]**.

The largest HR manufacturers include Indexator Rotator Systems AB, Heinz THUMM Ölhydraulische Antriebe GmbH, BALTROTORS Ltd and smaller manufacturers include Finn-Rotor Estonia Oü, AVS Hydraulikmotoren GmbH, Ahydraulics, Formiko Hydraulics Ltd.

A hydraulic rotator is a device that is part of a hydraulic grapple (grab) (Figure 1). The grapple is an additional piece of machinery that enables the material such as scrap metal, municipal waste, paper, sand, aggregate, ore, etc. to be gripped by means of claws (grippers). These claws (tines) are either in the form of two opposing spoons or by means of so-called polyp claws, which embrace the material and clamp it into a spherical shape.
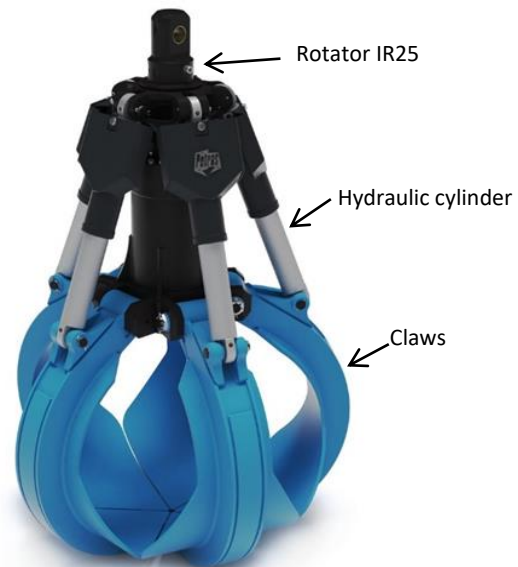

Figure 1. Metal scrap grapple (grab) with rotator Indexator IR25 [Hydraulika Petras 2022]

The hydraulic rotator allows infinite rotation while simultaneously closing or opening the grapple and transfers all loads induced by the lifting equipment, excavator, gantry crane, hydraulic arm, etc. The hydraulic rotator is therefore a self-supporting rotary inlet for pressurised fluids of various kinds, driven by a hydraulic motor which can rotate the rotary inlet and the equipment mounted on the rotator.

2 DESIGN OF ROTATOR TECHNICAL DIAGNOSTICS SYSTEM

The whole HR condition monitoring system can be seen as a collection of data needed for the overall multiparametric diagnostics of the rotator, see Figure 2.
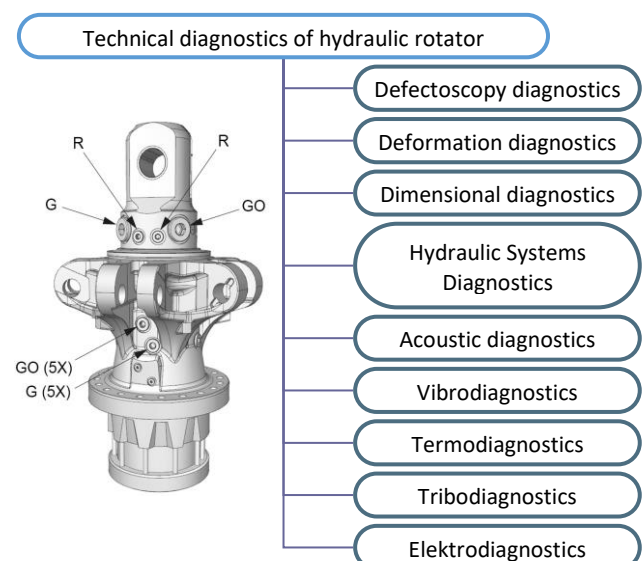

Figure 2. Technical diagnostics of hydraulic rotator IR25 [Indexator 2022]

The HR technical diagnostics system can include visual, defectscope, deformation, dimensional diagnostics, hydraulic system diagnostics, noise diagnostics, vibrodiagnostics, thermodiagnostics, tribodiagnostics and, for the latest rotators, even electrodiagnostics. [Hammer 2019], [Bosch Rexroth 2022], [Indexator 2022].

The purpose of defectoscopy is to determine the existence, location and size of material defects, both internal and surface. Defectoscopy diagnostics or non-destructive testing of HR primarily involves visual inspection of defects (cracks, broken HR parts, leaking grease around the main shaft, etc.), i.e. defects visible at first glance. In addition, defects can be inspected in this category using acoustic emission, magnetic, capillary, ultrasound, radiation (X-ray, radiation) methods, etc. [Hammer 2019], [Indexator 2022].

The deformation diagnostics consists of loading the HR in the axial direction and recording the deformation by tensometry (strain gauges) or any displacement of the main shaft and rotator body due to the load. Therefore, it is possible to consider the axial clearance in the IR 25 rotator as a suitable diagnostic parameter (see chapter 6.1. for more details).

Dimensional diagnostics in the evaluation of the HR condition is perceived as the inspection of the main dimensional parameters, inspection of the tolerances of the hinge parts, dimensional inspection of the flanges, input fittings, etc.

Diagnostics of the hydraulic system consists of inspection of the performance, efficiency, pressure loss, hydraulic rotator leakage, etc. [Deere 1997]. All values are calculated from static or dynamic changes in pressure, flow, and the actual speed of the hydraulic motor. In the case of HR, this is no-load rotation testing where the pressure drop of the hydraulic motor and its volumetric efficiency are evaluated. Next, the device is loaded with gradually increasing torque and its hydraulic parameters are again evaluated. From the rotation test results, a torque versus pressure drop chart can be determined with the important parameter of volumetric and overall efficiency at a given measured moment. From the hydraulic efficiency data, it is possible to effectively evaluate the technical condition within the life cycle of the hydraulic motor driving the HR (see chapter 6.2 and 6.3 for more details). Another parameter tested is the tightness of the rotary inlet. For illustrative purposes, Fig. 2 shows an IR25 rotator from the Swedish company Indexator, where R indicates the inlets for driving the hydraulic motor and G and GO indicate the passageways through the rotary inlet for closing and opening the grapple. Acoustic (noise) diagnostics uses the emission of sound energy from the HR as a carrier of information about its technical condition. These measurements are suitable for routine product noise inspection, development work, acoustic technical diagnostics [Nemecek 2012], [Ekosoftware 2022].

Rotator vibrodiagnostics can be used to inspection bearing functionality and hydraulic motor operation effectively. Because of the slow-speed machine measurements, an ultra-low frequency accelerometer such as the Model 731A with a P31 power amplifier system is required [Wilcoxon 2015]. For the measurement of Acoustic Emission Enveloping, e.g. the CMSS 786M sensor from the company SKF can be used [SKF 2022]. For more information on HR vibration measurement, see the article Vibration diagnostics on a hydraulic rotator [Budik 2015].

Thermodiagnostic measurement is a contactless HR temperature measurement that deals with the analysis of the temperature field distribution on the surface of the body. Thermal diagnostic evaluation using an infra-red camera allows to monitor the temperature of bearings and individual hydraulic channels, etc. [Stejskal 2009].

Tribodiagnostics (oil analysis), is used to determine the condition of the oil in terms of its lubricity and HR wear. The hydraulic rotator can be inspected for residual oil inside the hydraulic motor or online condition monitoring of the oil flowing through the chambers when testing HR. [Lundström 2017].

Electrodiagnostic monitoring of parameters has been introduced in recent years, when individual manufacturers have introduced an electric rotary input to rotators to drive various devices inside the grapple, e.g. remote diagnostics of grapples, integrated scale in the rotator, camera system [Hydraulika Petras 2022].

For the experiment, a total of 30 new HR IR25s manufactured between 2021 and 2022 were obtained. Four diagnostic parameters were used to evaluate their technical condition: the value of axial clearance in the rotator (rotator force tension in the axial direction), rotation testing without load and with torque load, and rotary inlet leakage testing.

3 PRINCIPLE OF IR25 ROTATOR FUNCTION

The principle of the function is explained on the IR25 rotator from the Swedish company Indexator. There are many variations of rotators where different types of drive hydraulic motors and different types of rotary inlets are used. For illustrative purposes, all measurements are made on this rotator. The IR25 rotator has a maximum diameter of 500 mm, height of 800 mm and a weight of 226 kg.
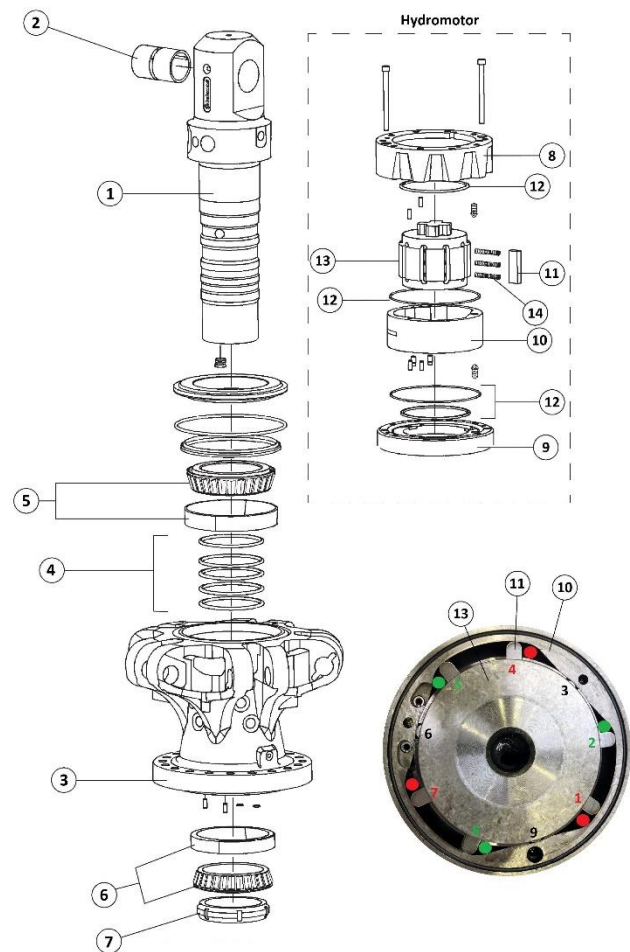

Figure 3. Rotator IR25 [Indexator 2022]

The IR25 rotator (Figure 3) has a maximum static load without rotation in the axial direction of ±450kN. When rotating, i.e. during dynamic loading, it is ±200kN and reaches a max. torque of 4100 N.m. This rotator is a device which consists of a main shaft (1) in which a hinged bronze bushing (2) is pressed. Next, a rotator body (3) into which a rotary inlet seal (4) is inserted.

The main shaft (1) is held in the rotator body (3) by a pair of opposing tapered roller bearings (5 and 6). All are tightened by a main central nut (7) to the prescribed torque.

The hydromotor is located at the bottom of the assembled rotator. The stator is composed of three parts, upper (8) and lower (9) flanges and a middle part (10) with an internal three-chamber shape for the vanes (11). The whole assembly is sealed by a set of seals (12).

The vane hydraulic motor contains nine vanes (11) and is three-chambered to achieve high torque. The vanes (11) are inserted in the rotor (13) and are pressed into the internal shape of the stator centre (10) by means of springs (14).

The pressure fluid is delivered to the point in front of the first, fourth and seventh vane (shown in red) and discharged from the point behind the second, fifth and eighth vane (shown in green), following the indicated direction of rotation. Due to the fact that the pressure is always applied to the surface of the three vanes, a pressure force is produced on these surfaces and converted into the required output torque of the rotator.

For the subsequent evaluation of the measurements, it is essential to have a thorough understanding of the principle of construction and function of each rotator under test.

4   CONSTRUCTION OF THE TEST BENCH

For the testing of the HRs and their subsequent assembly and disassembly, it was necessary to create an entire diagnostic centre for hydraulic rotators (Figure 5). Demands were placed not only on overall safety, the correct selection of a suitable crane, noise minimisation, assembly and dismantling fixtures, work tables, but also on all other relevant requirements for its features and functions, see Figure 6.   The individual requirements in this system approach form the basis for assessing the quality of the designed and implemented diagnostic centre [Janicek 2013], [Marek 2010].

The test bench (see. Figure 4) has all components designed to be able to carry a load in the axial direction of ±300 kN with the ability to simultaneously brake with a torque of ±4500 N.m.

The HR being tested can be cyclically loaded with these conditions in various combinations according to the defined conditions while pressurising the rotary inlet at a maximum pressure of 320 bar. The measurement results obtained with this device can be of great importance in the design of new rotators,
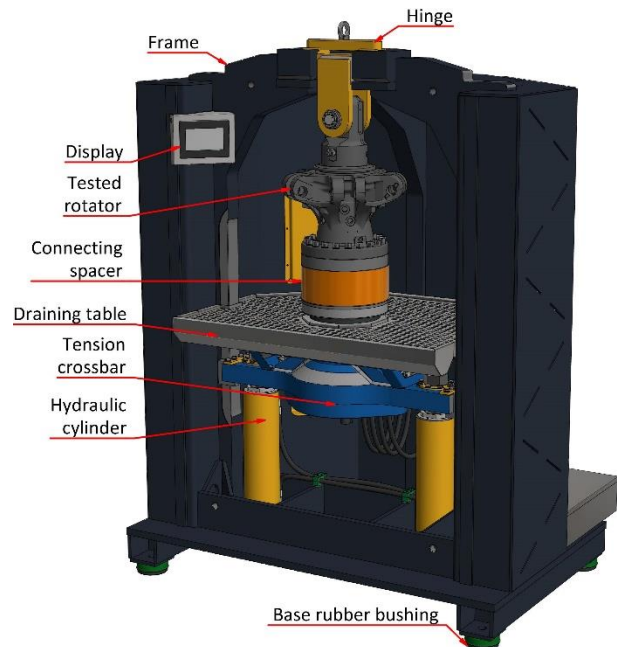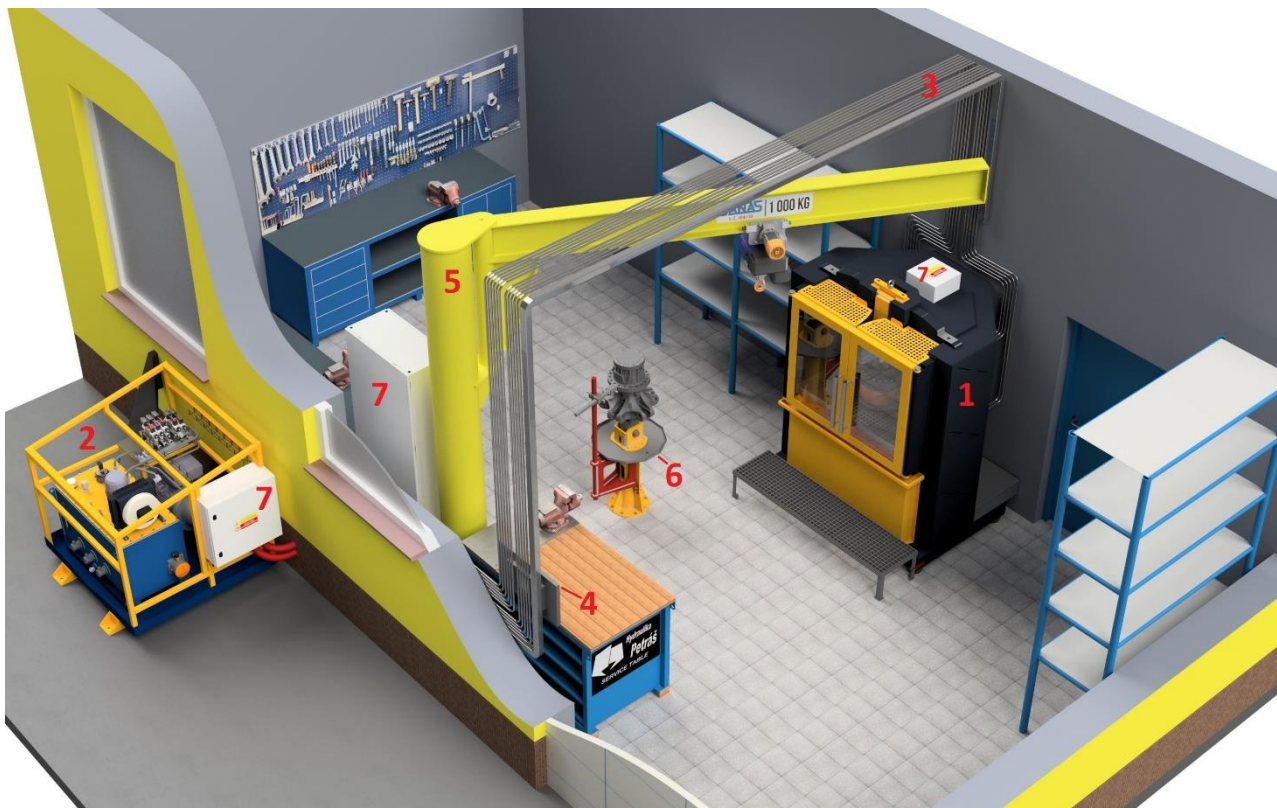
Figure 4. Individual parts of the test bench

1 - Test bench, 2 - Hydraulic unit, 3 - Hydraulic pipelines with electrical lines,
4 - Control panel, 5 - Rotary crane, 6 - Assembly jig, 7 - Electrical switchboards

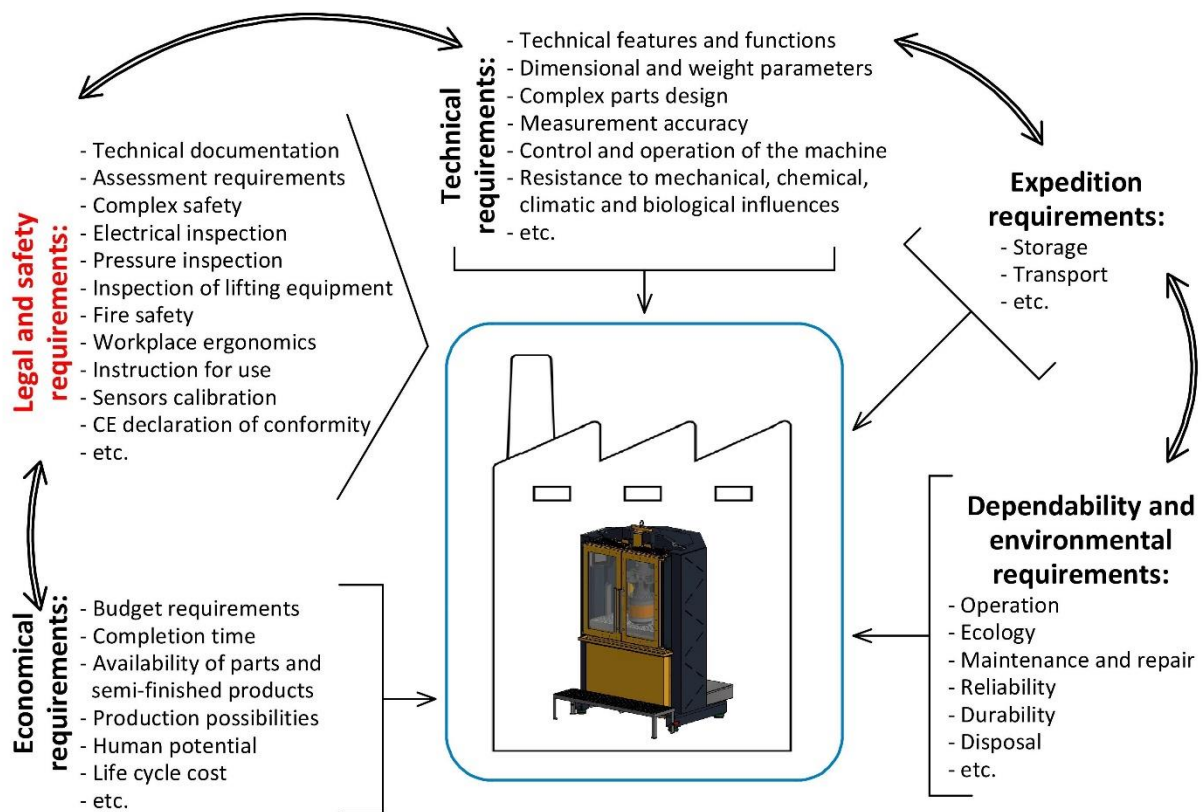**Figure 5.** Diagnostic centre for hydraulic rotators

Figure 6. Requirements for hydraulic rotators diagnostic centre

in the verification of the functionality of prototypes and in the inspection of condition of rotators after repair.

This article further describes only the test bench itself (Figure 4), where the main parts of the test bench are listed. The basic part of the test stand is a composite reinforced concrete frame with a total weight of 4500 kg. At the top there is a hinge on which various rotators are mounted. Below the rotator is an interchangeable spacer for connection to the torque brake. The draining table collects the waste oil from the assembly and disassembly of the tested rotators. A pair of straight hydraulic motors, located at the bottom of the machine, provide the required axial force to tension the rotator. These hydromotors have position metering built into them and are controlled in either force or position feedback. They are loose in the bottom and top in spherical plain bearings to eliminate mutual deformation.

Two hydraulic motors are built into the crossbar for braking or, conversely, for positioning the connecting spacer. This system is again controlled in feedback to the position determined by the rotary encoder located at the bottom of the crossbar.

In manual mode, the current position values are shown on the display. For initial positioning, a handwheel is used, which can change the height position of the table or the rotation of the connecting spacer after specified increments. In the automatic mode, the actual measurement of the technical parameters of the HR is carried out according to the created measurement programme.

The entire test bench is placed on the base of the silent blocks to minimize the transmission of vibrations from the surroundings. In order to create suitable laboratory conditions, the 35kW hydraulic power unit had to be located outside the test room. Figure 7 shows a realistic view of the inside of the test bench with the IR 25 rotator clamped and ready for testing.

5 SHEWHART CONTROL CHARTS

In order to be able to investigate the condition of each technical parameter, it was necessary to introduce systematic statistical data processing. For this purpose, a control chart for individual values and a moving range was chosen. The control chart is a tool for statistical process control SPC (Statistical Process Control). A control chart is a graphical means that is used to show changes in a process or its key metrics over time. This chart always has a Central Line (*CL*) and Upper Control Limit (*UCL*) and Lower Control Limit (*LCL*), the so-called action limits, which are either derived from historical data or are a target value determined by regulation. From the time course of the diagram, it is possible to conclude whether the behavior of a process or diagnostic parameter is in the state of statistical control or whether it is unpredictable (out of control) **[Tosenovsky 2000]**.

In our case, for the statistical control of the HR technical inspection process, Shewhart control charts are used to determine the lower and upper control limits of each measured parameter, generally for each type of new or repaired rotator. Thus, it can be said that each measurand has its expected range determined by the lower and upper control limits within which the measured values are to be located (with a probability of 99.73%).

Figure 7. Inner part of the test bench with hydraulic rotator IR25

5.1 Control charts for individual x_i values

In this type of control chart, the individual measured values x_i (i = 1, 2,... n) are recorded. The central line is therefore equal to the arithmetic mean $\bar{x}$ of all measured values.

$$CL_x = \bar{x} = \frac{\sum_{i=1}^{n} x_i}{n} \qquad (1)$$

The upper and lower control limits for x_i are generally calculated according to the following formula:

$$UCL_x = \bar{x} + 3\sigma, \qquad (2)$$
$$LCL_x = \bar{x} - 3\sigma, \qquad (3)$$

where σ is the standard deviation of the population, estimated by using average moving range:

$$\hat{\sigma} = \frac{\bar{R}_k}{d_2} = \frac{\bar{R}_k}{1.128}, \qquad (4)$$

where d_2 is Hartley's constant, now for the sample size "2": d_2 = 1.128 see Table 2 in the standard [CSN ISO 7870-2:2018]. $\bar{R}_k$ is the average moving range, which we calculate according to equation:

$$\bar{R}_k = \frac{\sum_{l=1}^{n-1} R_{k_l}}{n-1}, \text{ where} \qquad (5)$$

$$R_{k_l} = |x_l - x_{l+1}|. \qquad (6)$$

Substituting (4) into relations (2) and (3) we get:

$$UCL_x = \bar{x} + 3\frac{\bar{R}_k}{d_2} = \bar{x} + 2.66\bar{R}_k, \qquad (7)$$

$$LCL_x = \bar{x} - 3\frac{\bar{R}_k}{d_2} = \bar{x} - 2.66\bar{R}_k. \qquad (8)$$

5.2 Control chart for the moving range R_k

The control chart for the moving range R_k is intended to monitor the values of the individual moving ranges R_{k_l}.

We define the value of the central line CL_{R_k} in terms of the magnitude of the average moving range $\bar{R}_k$ according to relation (5) mentioned above.

To determine the control limits in the control chart for the moving range, we use equations:

$$UCL_{R_k} = \bar{R}_k + 3\sigma_{R_k} = \bar{R}_k + 3d_3\frac{\bar{R}_k}{d_2} =$$
$$\left(1 + \frac{3d_3}{d_2}\right)\bar{R}_k = D_4\bar{R}_k = 3.267\bar{R}_k, \qquad (9)$$

$$LCL_{R_k} = \bar{R}_k - 3\sigma_{R_k} = \bar{R}_k - 3d_3\frac{\bar{R}_k}{d_2} =$$
$$\left(1 - \frac{3d_3}{d_2}\right)\bar{R}_k = D_3\bar{R}_k = 0. \qquad (10)$$

In the standard [CSN ISO 7870-2:2018] and in the last modification of relation (9), the expression $\left(1 + \frac{3d_3}{d_2}\right)$ is replaced by D_4 and in relation (10) the expression $\left(1 - \frac{3d_3}{d_2}\right)$ is replaced by D_3. For the moving range, the symbols have the values D_4 = 3.267 a D_3 = 0 see Table 2 in the standard [CSN ISO 7870-2:2018].

6 EXPERIMENTAL MEASUREMENT OF THE TECHNICAL CONDITION OF ROTATORS

In this chapter, four diagnostic parameters were used to evaluate the technical condition of the hydraulic rotator IR25 from the Indexator company. A modified Shewhart control chart method is used to evaluate the values of individual parameters for individual values and moving ranges. The modifications are that we do not have a real series of 30 consecutive rotators, but variously mixed according to the deliveries from Indexator. Therefore, some of the 8 tests for assignable causes have a modified meaning. Another modification is to create an auxiliary control chart from the eight volumetric efficiency control charts.

The following chapters use the technical units that are used by manufacturers and in engineering practice.

6.1 Testing the axial rotator clearance

The principle of this measurement is to load the IR25 rotator in axial direction by first compressing it with a force of 100kN and then stretching it with a force of 200kN. During this load change, the dimensional change between the rotator body and the main shaft is recorded in the measuring system. This measurement is carried out by means of a digital length indicator located on the rotator body.

The 30 new IR25 rotators were measured and from the values a Shewhart control chart was created for the individual values and for the moving range (see Figures 8 and 9) [ČSN ISO 7870-2:2018].

All measured values were in the range of 105-130 μm and these values resulted in an average of 117.1 μm with a sampling standard deviation of 6.3 μm and an average moving range of 8.1 μm.

Figure 8 shows the control chart for individual axial clearance values with the measured values plotted and the calculated control limits UCL_{AC}= 139 μm, LCL_{AC}=96 μm and the central line CL_{AC}=117.1 μm.
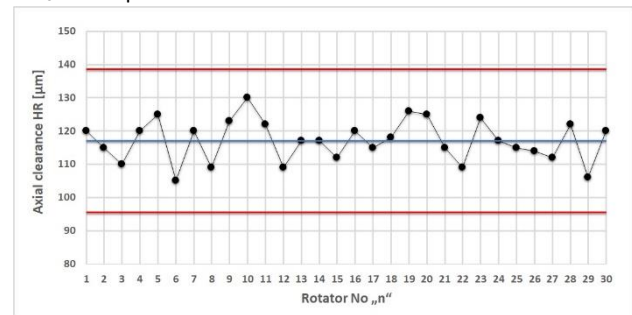

Figure 8. Control chart for individual values of axial clearance IR25 rotators with control limits

An integral part of the control chart for individual values is the control chart for the moving range Figure 9, which tracks the range of consecutive measurements. The calculated limits for the moving range of axial clearance are $UCL_{R_{k-AC}} = 26.4\ \mu m$ and the central line $CL_{R_{k-AC}} = 8.1\ \mu m$.
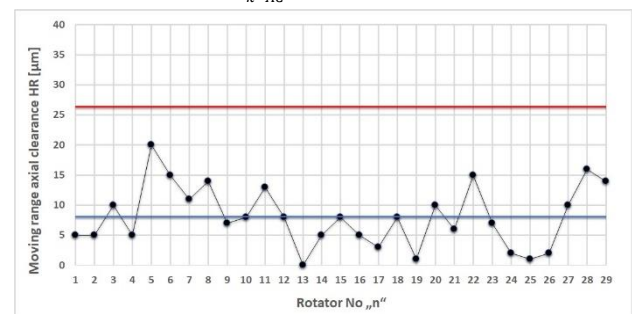

Figure 9. Control chart for the moving range of axial clearance IR25 rotators with control limits

Both control charts confirm the process is in statistical control for the individual values and the moving range.

These diagrams can be used in two ways. The first way is series production, where we enter new measurements into the chart during production to find out if the process is in statistical control (in terms of axial clearance requirement). From these measurements, in series production, a so-called production sheet of the measured parameter is created, in which we can see any temporal destabilisation of the production process and can intervene in time. The second way of application is to use these control charts to inspect the pieces being repaired (or to evaluate the condition of the rotator before repair).

Table 1 shows the individual axial clearances of the IR25 rotator where the column is mounted in two opposing tapered roller bearings preloaded by a central nut inside the rotator.

Rotator type	Number of hours in operation	Axial clearance [μm]
IR 25	cca. 1000	140
IR 25	cca. 2100	155
IR 25	cca. 3500	190

Table 1. Table used rotators of axial clearances

From the table it is possible to read the changes in axial clearance over the lifetime of the rotator and, if sufficient data is collected, its actual life cycle can be predicted in interaction with other parameters. As rotators belong to the category of hanging equipment, this test is very important from a safety point of view. Rotators are most commonly used on excavators where there is not a high risk of damage to other property or risk of personal injury if the rotator should break off. Another possible use is on trucks where the grapples are hung from hydraulic arms and there is a high risk of damage to other property or risk of personal injury if the rotator is torn off due to poor assembly or wrong tightening of the central nut.

6.2 Testing HR rotation without torque load

Torque-free rotation testing is a dynamic process of inspection the functionality of the hydraulic motor that powers the rotator. In this process, two parameters are proposed to be monitored, the pressure drop at the hydraulic motor Δp [bar] and the volumetric efficiency η_v [%].

The pressure drop determines the torque load on the hydraulic motor M [N.m] reduced by the hydromechanical efficiency value η_{hm} [%]. For the overall hydraulic efficiency η_c [%], which is used to calculate the real performance of the hydraulic motor, the following applies (efficiency values are in decimal numbers):

$$\eta_c = \eta_v \cdot \eta_{hm}. \tag{11}$$

The torque load on the hydraulic motor is calculated according to the following relation:

$$M = \frac{V_g \cdot \Delta p}{20 \cdot \pi} \cdot \eta_{hm}, \tag{12}$$

where the value of the geometric volume V_g enters the equation [cm³], where for our IR25 rotator this value is 1314 cm³ **[Cerha 2009]**, **[Indexator 2022]**.

No-load HR rotation testing means that the output torque is zero, so the hydromechanical efficiency also equals zero. It is therefore important to note that the pressure drop measured on the hydraulic motor during free rotation is equal to the torque required to overcome any mechanical losses such as bearing rolling resistance, rotary inlet resistance, etc.

For the 30 new IR25 rotators, the average pressure drop at a constant flow rate of 10 dm³.min⁻¹ through the hydraulic motor was 48.6 bar with a standard deviation of 2.6 bar and an average moving range of 2.8 bar.
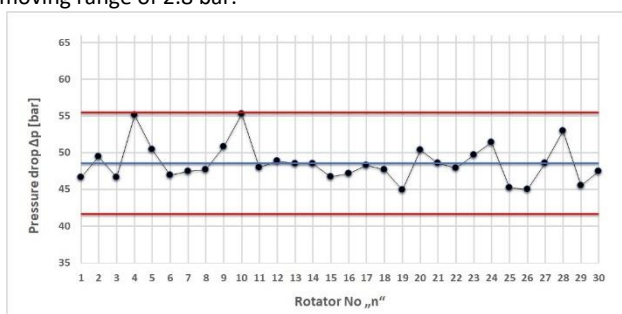

Figure 10. Control chart for individual pressure drop values of IR25 rotators at constant flow rate of 10 dm³.min⁻¹

Figure 10 shows the control diagram for the individual values of the pressure drops of the new IR25 rotators with the calculated limits $UCL_{\Delta p}$= 55.5 bar, $LCL_{\Delta p}$=41.7 bar and the central line $CL_{\Delta p}$=48.6 bar.

When evaluating the control chart, it is also necessary to monitor the control chart for the moving range at the same time (Figure 11). The calculated limits for the moving range pressure drop are $UCL_{R_{k-\Delta p}} = 9.2\ bar$ and the central line $CL_{R_{k-\Delta p}} = 2.8\ bar$.
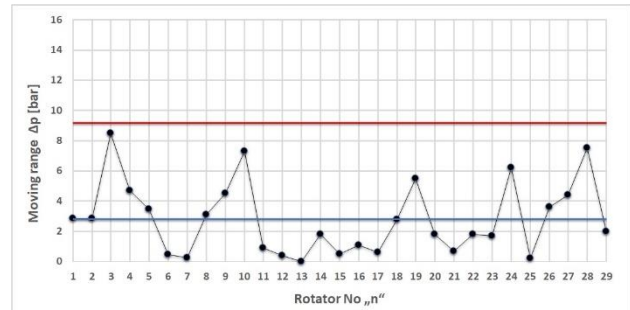

Figure 11. Control chart for the moving range pressure drop of IR25 rotators at a constant flow rate of 10 dm³.min⁻¹

The equation (12) implies that the rotator itself (if the seals, bearings, hydraulic motor, manufacturing tolerances are correct etc.) requires approximately 1016 N.m for rotation itself with ignoring the hydromechanical efficiency of the hydraulic motor itself.

The control charts in Figures 10 and 11 confirm the process is in statistical control for the individual values and the moving range (in terms of pressure drop of IR25 at a constant flow rate of 10 dm³.min⁻¹). In the case of incorrect assembly, poor sealing, excessive main shaft or poor manufacturing tolerances, the values of pressure drop will be outside the calculated limits and the rotator will need to be repaired.

The second parameter that characterizes the quality and condition of the hydraulic motor driving the HR is the volumetric efficiency η_v. It is parameter that indicates in % how much fluid is released by the hydraulic motor without being used. Thus, for the volumetric efficiency of the hydraulic motor applies:

$$\eta_v = \frac{V_g \cdot n_H}{1000 \cdot Q_H}, \tag{13}$$

where Q_H [dm³.min⁻¹] is the input flow to the hydraulic motor and n_H [1.min⁻¹] is the actual output speed of the rotator. The condition for measurement and comparison of volumetric efficiencies is to measure at constant oil temperature, i.e. constant viscosity **[Cerha 2009]**. The temperature during our measurement was 50°C ±3°C.

Pressure drop measurement and volumetric efficiency measurement on the test stand is a fully automated measuring process, where the operator simply hangs the rotator and connects the supply hoses to the rotator. To achieve an automatized process, it is necessary to obtain the real speed of the hydraulic motor from the time record of the pressure drop. For this purpose, the mathematical method of the discrete Fourier transform is used **[Tuma 1997]**. Using this method on the time record of pressure we obtain the frequency spectrum from which we can read, among other things, the rotational frequency and the correct function of the individual vanes in the hydraulic motor.

Figure 12 shows a time record of the pressure, where the blue colour shows the actual pressure waveform and orange shows the filtered signal of the two main frequencies. Thus, the rotation frequency of the rotator and the frequency of the particular pressure shocks that cause the vanes during rotation by the hydraulic motor. In Figure 13, these two frequencies are also shown in orange colour in the frequency spectrum.

For illustration and simplicity, the frequency spectrum has x-axis converted to period. Thus, from the periodic spectrum we can say that the rotation period of the rotator is 9.45s (0.105 Hz) and the lamellar period is 1.05s (0.95 Hz).
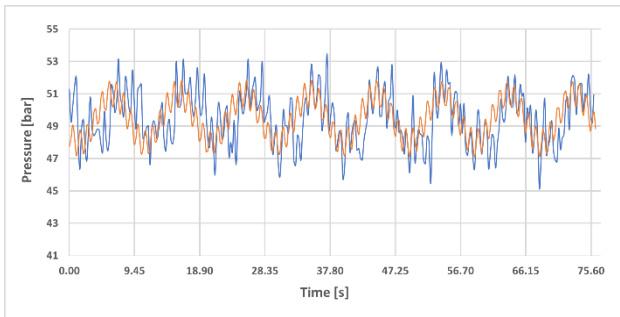

Figure 12. Time record of the pressure drop on the hydraulic motor of the rotator IR25 at a constant flow rate of 10 dm³.min⁻¹

Due to the fact that the hydraulic motor has 9 vanes, then nine times the vane period is exactly the rotation period of the rotator, which is 9.45s.
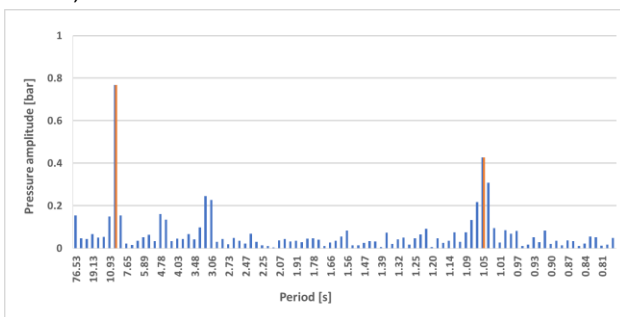

Figure 13. Frequency spectrum of the pressure drop on a hydraulic motor of the IR25 rotator at a constant flow rate of 10 dm³.min⁻¹

In the event of a failure of the hydromotor, the time record is distorted and the rotation period is no longer consistent with the multiple of the lamellar frequency. Thanks to this analysis of the time record, it can be clearly determined the speed of each measured rotator and again create Shewhart's control charts of the individual volumetric efficiencies from the 30 new IR25 rotators.

Figure 14 shows the control chart for the individual values of volumetric efficiencies at constant flow 10 dm³.min⁻¹ for the new IR25 rotators with calculated limits $UCL\eta_{v1}$= 88 %, $LCL\eta_{v1}$=79.5 % and the central line $CL\eta_{v1}$=83.8 %.
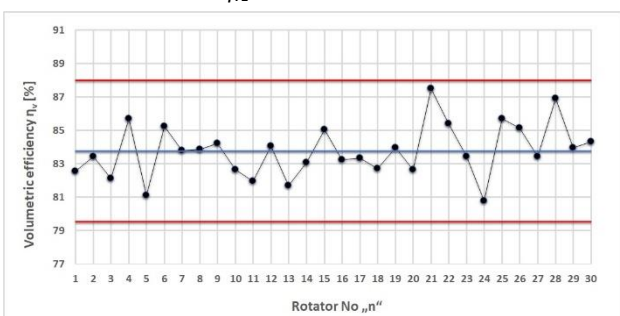

Figure 14. Control chart for individual values volumetric efficiency on the IR25 rotator at a constant flow rate of 10 dm³.min⁻¹

Figure 15 shows the limits for the moving range in a graph of volumetric efficiencies $UCL_{R_{k-\eta v1}} = 6.4\ bar$ and the central line $CL_{R_{k-\eta v1}} = 2\ bar$.

In the case of damage to the vanes due to oil contamination or breakage of the compression spring or other mechanical damage, the volumetric efficiency is greatly reduced. These cases of damage occur in approximately 5 - 7% of rotators that are repaired **[Indexator 2022], [Hydraulika Petras 2022]**.

These values of volumetric efficiencies are taken as the highest possible for a given flow rate and also as a baseline for further measurements, where the volumetric efficiency will gradually decrease with increasing load moment, i.e. increasing pressure drop on the hydraulic motor.
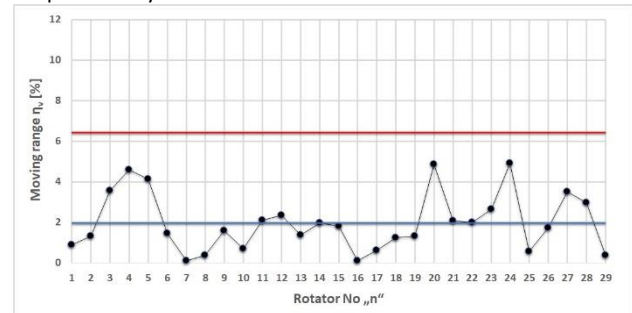

Figure 15. Control chart for the moving range of volumetric efficiency on the IR25 rotator at a constant flow rate of 10 dm³.min⁻¹

Figures 14 and 15 confirm the process is in statistical control for the individual values and the moving range (in terms of volumetric efficiency at a constant flow rate of 10 dm³.min⁻¹).

6.3 Testing HR rotation with torque load

In the previous measurement, the rotator was only fixed by a hinge at the top of the measuring stand and could rotate freely. In order to test the rotator by torque, it is necessary to connect the rotator in a fixed connection with the tensioning crossbar, see figure 16. The crossbar has two hydraulic motors in it, which brake or drive the rotor located in the middle of the crossbar, and is firmly connected to the rotator by means of the connecting spacer.

Figure 16. Section through the tensioning crossbar of the test stand

The principle of measurement is based on the gradual loading of the HR moment. For our first measurement, it was proposed to drive the HR hydraulic motor at a constant flow rate of 10 dm³.min⁻¹, at a relatively constant temperature of 50°C ± 5°C. The result of loading the HR at constant flow rate is always a slowing down of the HR speed (decrease in volumetric efficiency), which is recorded in the graph. The volumetric efficiencies were automatically recorded as the pressure drop values from 60 to 120 bar were reached in increments of 10 bar.
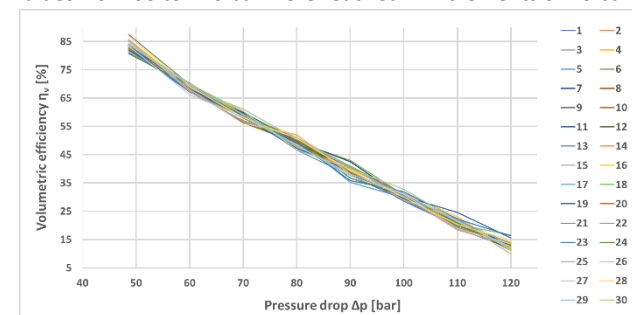

Figure 17. Measurement of volumetric efficiencies of 30 HRs under torque loading

Again, 30 pcs of new rotators were measured and these measurements are plotted in the graph in Figure 17 to illustrate the measured data.

From the measured values, 8 Shewhart control charts were created for pressure drop of 48.6, 60, 70, 80, 90, 100, 110, 120 bar. From these control charts an auxiliary chart was created, (see Figure 18) where the *UCL* and *LCL* waveforms are shown under HR torque loading.
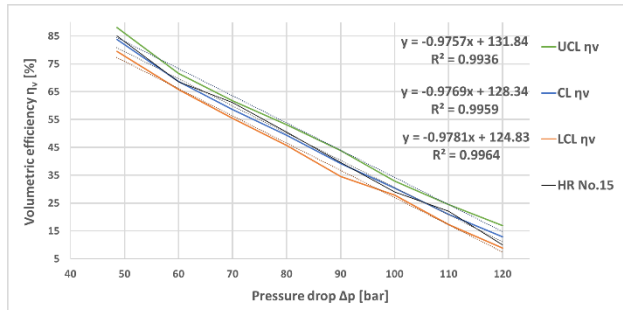

Figure 18. Control chart for the individual values of the volumetric efficiencies of 30 HRs under torque loading

When these diagrams are combined, they produce graphs where the *UCL* and *LCL* are variable and do not just represent a horizontal line in the graph at a certain value. The variable boundaries are shown in the graph in Figure 18. for individual values. Thus, from the graph, after linear approximation of the graph, we can say that the graph can be plotted with boundary conditions for $x \in \langle 48.6 ; 120 \rangle \; bar$:

$$UCL^*_{\eta v} = -0.98x + 131,84 \; [\%],$$
$$CL^*_{\eta v} = -0.98x + 128,34 \; [\%],$$
$$LCL^*_{\eta v} = -0.98x + 124,83 \; [\%].$$

6.4 Leak testing of the rotary inlet in HR

Rotary inlet testing consists of pressurizing the closed circuits and monitoring the pressure change over time while the rotators rotate. In Fig. 17, the graph shows two rotators, with one being brand new and the other having been in operation for approximately 2500 hours.
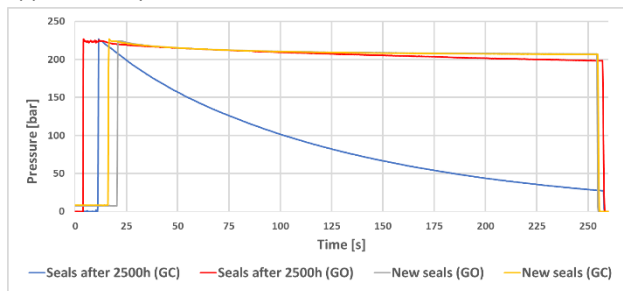

Figure 19. Time record of pressure drop of pressurized rotary inlet

The curves in grey and yellow are almost covered and are the closing and opening branches of the new rotator. The pressure drop after stabilization is almost zero in time and is only due to the leakage of the electromagnetic seat hydraulic valves located in the hydraulic power unit manifold, which is approximately 1 bar.min^{-1} in this built-in assembly.

The curves marked in red and blue are examples of a damaged rotary inlet seal. The blue curve shows the closing branch of the grapple, which is much more stressed by impact pressure changes than the opening branch, marked in red in the graph. The leakage on the closing branch (approx. 50 bar.min-1) is also visible on the outer casing of the rotator, where this defect is manifested by oil leakage around the main shaft. The second opening branch is an example of damage or wear of the sealing elements to the extent that it is still functional (pressure drop of approx. 6 bar.min-1), but in a very short time the same damage as on the closing branch would occur. When testing the tightness of the rotary inlets, special care must be taken to watch out for these small leaks, which lead to early complete dysfunction of the entire grapple.

The data collection for the control chart is carried out after the pressure has been stabilized by closing the pressurized part. This means that after a period of 120s, the pressure value is recorded and then a second pressure value is recorded after 60s. The difference of these pressures is the pressure drop in 1 minute after the initial pressure stabilisation.

Figure 20 shows the control chart for individual values of the pressurized rotary inlet for 60 s with measured values and calculated limits $UCL_{60-\Delta p}$= 1.82 bar, $LCL_{60-\Delta p}$ =1.31 bar as well as the central line $CL_{60-\Delta p}$ =1.57bar.
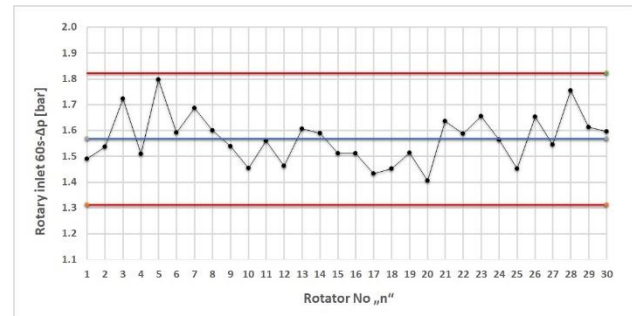

Figure 20. Control chart for individual values of pressure drop during leak testing

Figure 21 plots the calculated values of the moving range and the boundary representation for the moving range of the pressurized rotary inlet $UCL_{R_{k-60\Delta p}} = 0.36 \; bar$ and the central line $CL_{R_{k-60\Delta p}} = 0.11 \; bar$.
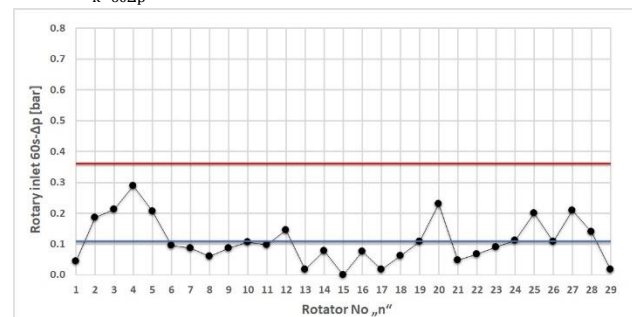

Figure 21. Control chart for the moving range pressure drop during leak testing

Figures 20 and 21 confirm the process is in statistical control for the individual values and the moving range (in terms of leak testing rotary inlet).

7 CONCLUSIONS

In this paper, a system of technical diagnostics of hydraulic rotators is designed as a set of 9 types of technical diagnostics, which consists of visual diagnostics, defectoscopic, deformation, dimensional, hydraulic system diagnostics, acoustic diagnostics, vibrodiagnostics, thermodiagnostics, tribodiagnostics and electrodiagnostics.

Based on the analysis of the construction and function of the available types of hydraulic rotators offered on the world market, a system of requirements for the design of a hydraulic rotator diagnostic centre was developed. The individual requirements have been organized into 5 groups, which are made up of legal and safety requirements, technical requirements, economic requirements, dependability and environmental requirements and delivery requirements.

The diagnostic centre development was started in 2015 and was completed in June 2022. The cost of the development reached almost 10mil. CZK and the diagnostic centre is now in trial operation.

	Diagnostic parameter	UCL_{xi}	LCL_{xi}	CL_{xi}	UCL_{Rk}	LCL_{Rk}	CL_{Rk}
1	Axial clearance [um]	139	96	117.1	26.4	0	8.1
2	Without load Δp [bar]	55.5	41.7	48.6	9.2	0	2.8
3	Without load (48.6 bar) η_{v1} [%]	88.0	79.5	83.8	6.4	0	1.97
	With load (60 bar) η_{v2} [%]	71.5	65.7	68.6	4.0	0	1.23
	With load (70 bar) η_{v3} [%]	61.7	55.4	58.6	4.3	0	1.30
	With load (80 bar) η_{v4} [%]	53.2	45.7	49.4	5.1	0	1.57
	With load (90 bar) η_{v5} [%]	43.9	34.5	39.2	6.6	0	2.03
	With load (100 bar) η_{v6} [%]	32.8	27.8	30.3	3.3	0	1.00
	With load (110 bar) η_{v7} [%]	24.5	17.3	20.9	5.4	0	1.64
	With load (120 bar) η_{v8} [%]	16.9	8.9	12.9	5.0	0	1.53
4	Leak testing (60s) Δp [bar]	1.82	1.31	1.57	0.36	0	0.11

Table 2. Summary table of control limits for individual diagnostic parameters

The most important element of the test centre is the test bench, which is able to test selected types of rotators with maximum load parameters in the axial direction of ±300 kN with the possibility of simultaneous braking torque of ±4500 N.m.

The experimental measurements were carried out on a total of 30 new IR25 hydraulic rotators manufactured by the company Indexator in the years 2021-2022. To evaluate their technical condition, four diagnostic parameters were used, which included the value of axial rotator clearance (at a defined force tension of the rotator in the axial direction), testing the pressure drop and the volumetric efficiency of the hydraulic rotator. The fourth parameter was testing the rotary inlet leakage after pressurization with the prescribed pressure. For the evaluation of measured values, modified Shewhart control charts for individual values of diagnostic parameters and their moving ranges were designed. Table 2 above shows the values of the central lines, upper and lower control limits of the four diagnostic parameters.

In the first line, the control limits for the values of the rotator axial clearance are given, which involves the evaluation of the dimensional change between the rotating body of the rotator and its main shaft after its compression with a force of 100 kN and subsequent stretching with a force of 200 kN in the test bench. In terms of the control charts, measured values of dimensional change from 96 to 139 μm can be expected, which were calculated from measured values in the range of 105-130 μm.

The second line shows the control charts for the pressure drop of the hydraulic motor that drives the IR25 hydraulic rotator at a constant flow rate of 10 dm³.min⁻¹. For the new rotator, values from 41.7 to 55.5 bar can be expected, which were calculated from the measured values.

In the third line, the control limits for the volumetric efficiency values (at a constant flow rate of 10 dm³.min⁻¹) for the pressure drop of the hydraulic motor 48.6, 60, 70, 80, 90, 100, 110, 120 bar are successively given. The value of 48.6 bar corresponds to the no-load condition of the hydraulic rotator.

The last line shows the control charts for the pressure drop values after pressurizing the rotary inlet to 230 bar for 180s. The pressure drop is evaluated as the difference of the measured pressures at 180s and 120s.

The conducted measurements proved the full functionality of the created test centre including the unique test bench. And the calculated values of the control charts for the selected diagnostic parameters make it possible to distinguish the good technical condition of the new hydraulic rotators from the unacceptable technical condition. The main contribution is the development of a system to evaluate the technical condition of the rotator using four justified parameters for which limit values have been defined. The use of control charts provides an important tool for assessing the quality of different types of rotators and comparing the quality of rotators from different manufacturers. The information provided can also be used effectively to assess the quality of repairs carried out on hydraulic rotators.

The authors expect the following research to continue in the next period:

- conducting further measurements and creating control charts for individual parameters for other types of hydraulic rotators, e.g. from Indexator Rotator Systems AB, Heinz THUMM Ölhydraulische Antriebe GmbH, BALTROTORS Ltd, etc.,
- the creation of control charts for the maximum permitted values of constant flow rates,
- adding equipment to the test bench to include instrumentation for torque and vibration measurements (after obtaining the necessary funding),
- evaluating the capability of the test bench as measuring system and the measurement process for each diagnostic parameter.

ACKNOWLEDGMENTS

REFERENCES

Book:

[Cerha 2010] Cerha, Josef. Hydraulic and pneumatic mechanisms I. Liberec: TU v Liberci, 2010. ISBN 8073725600. (in Czech)

[Dell 2015] Dell, Tim and Dell, Timothy W. Hydraulic Systems for Mobile Equipment. Chicago: Goodheart-Willcox Publisher, 2015. ISBN 1631264141.

[Deere 1997] Deere, John. Hydraulic Systems Diagnostics. Moline: Deere & Co, 1997. ISBN 0866912495.

[Gotz 1998] Gotz, Werner. Hydraulics: Theory and Application. Ditzingen: Robert Bosch GmbH, 1998. ISBN 0768002427

[Janicek 2013] Janicek, Premysl and et al. Expert engineering in a system concept. Praha: Grada Publishing a.s., 2013. ISBN 9788024741277. (in Czech)

[Khalil 2016] Khalil, Medhat. Hydraulic Systems Volume 1: Introduction to Hydraulics for Industry Professionals. Milwaukee: Compudraulic LLC, 2016. ISBN 0692622365.

[Marek 2010] Marek, Jiri. Integrated product development. Praha: H. L. Production, 2010. ISBN 9788025464977. (in Czech)

[Singh 2017] Singh, K. Hiraniya. Pneumatic and Hydraulic Systems. Delhi, India: I. K. International Publishing House Pvt. Ltd, 2017. ISBN 9789385909337.

[Stejskal 2009] Stejskal, Tomas and Valencik, Stefan. Technical diagnostics. Košice: Strojnícka fakulta, TU v Košiciach, 2009. ISBN 9788055303130.

[Tosenovsky 2000] Tošenovsky, J. and Noskievičová, D. Statistical methods for quality improvement. Ostrava: Montanex, 2000. (in Czech)

[Tuma 1997] Tuma, Jiri. Signal processing of signals obtained from mechanical systems using FFT. Praha: Sdelovaci technika, 1997. ISBN 8073725600. (in Czech)

[Vacca 2021] Vacca, Andrea. Hydraulic Fluid Power: Fundamentals, Applications, and Circuit Design. New Jersey: Wiley, 2021. ISBN 9781119569107.

[Zhang 2019] Zhang, Qin. Basics of Hydraulic Systems, Second Edition. United Kingdom of Great Britain: Taylor & Francis Ltd, 2019. ISBN 9781138484665.

Technical standards

[CSN ISO 7870-2:2018] Control charts - Part 2: Shewhart control charts. Praha: UNMZ, 2018. (in Czech)

Technical reports or thesis:

[Hammer 2019] Hammer, M., Jankovych, R. and et al. Measurement Report II Design of Metrological Diagnostic Parameters. Brno: Fakulta strojiího inzenyrstvi. 2019. (in Czech)

[Lundström 2017] Lundstrom, Jonathan and Hörnberg, Emiluthor. Rotator assembly at Indexator. Lulea: Department of Engineering Sciences and Mathematics, 2017.

[Onderka 2014] Onderka, Tomas. Testers - hydraulic oil testing: Argo-Hytos Protech, 2014. (in Czech)

Paper in electronic journal:

[Budik 2015] Budik, Tomas and et al. Vibration diagnostics on a hydraulic rotator [online]. 2015. Available from <https://www.mmscience.eu/journal/issues/december-2015/articles/vibration-diagnostics-on-a-hydraulic-rotator>. DOI:10.17973/MMSJ.2015_12_201557

WWW page:

[Argo-Hytos 2022] Argo-Hytos. 2022, [online]. [5.8.2022]. Available from <http://www.argo-hytos.com/>.

[Argo-Hytos Protech 2022] Argo-Hytos Protech. 2022, [online]. [5.8.2022]. Available from <http:// http://www.hytosost.cz/>.

[Bosch Rexroth 2022] Bosch Rexroth. 2022, [online]. [5.8.2022]. Available from <http://www.boschrexroth.com/>.

[Ekosoftware 2022] Ekosoftware. 2022, [online]. [5.8.2022]. Available from <https://www.ekosoftware.cz/mereni-zvuku>.

[Hydac 2022] Hydac. 2022, [online]. [5.8.2022]. Available from <http:// www.hydac.com/>.

[Hydraulika Petras 2022] Hydraulika Petras. 2022, [online]. [5.8.2022]. Available from <http://www.hydraulikapetras.cz/>.

[Hycom 2022] Hycom B.V. 2022, [online]. [5.8.2022]. Available from < https://www.mhhydraulics.com/en/contact-us.html >.

[MH Hydraulics Netherlands 2022] MH Hydraulics Netherlands B.V. 2022, [online]. [5.8.2022]. Available from <https://hycom.nl/aviation-oud__trashed/hycom-aviation-test-benches/>.

[Nemecek 2012] Nemecek, P. Acoustic diagnostics, [online]. [5.8.2022]. Available from < http://www.kvm.tul.cz/getFile/id:1848/In-TECH%202_%20Akusticka_diagnostika.pdf>. (in Czech)

[Indexator 2022] Indexator. 2022, [online]. [5.8.2022]. Available from <http://www.indexator.se/>.

[SKF 2022] SKF. 2022, [online]. [5.8.2022]. Available from <http://www.skf.com/>.

[Wilcoxon 2022] Wilcoxon. 2022, [online]. [5.8.2022]. Available from < http://www.wilcoxon.com/ >.

CONTACTS:

Ing. Tomas Budik

Faculty of Mechanical Engineering, Brno University of Technology, Institute of Production Machines, Systems and Robotics

Technicka 2896/2. Brno, 616 69. Czech Republic

Telephone: +420 737 533 172, e-mail: budik@fme.vutbr.cz

doc. Ing. Robert Jankovych, CSc.

Faculty of Mechanical Engineering, Brno University of Technology, Institute of Production Machines, Systems and Robotics

Technicka 2896/2. Brno, 616 69. Czech Republic

Telephone: +420 605 440 420, e-mail: jankovych@fme.vutbr.cz